Available online at www.sciencedirect.com

ScienceDirect

Biochimica et Biophysica Acta 1767 (2007) 509–519

Biochimica et Biophysica Acta BBA

www.elsevier.com/locate/bbabio

Lipids in photosystem II: Interactions with protein and cofactors

Bernhard Loll [a,1], Jan Kern [b,*], Wolfram Saenger [a], Athina Zouni [b], Jacek Biesiadka [a]

[a] *Institut für Chemie und Biochemie/Kristallographie, Freie Universität Berlin, Takustr. 6, D-14195 Berlin, Germany*

[b] *Institut für Chemie/Max Volmer Laboratorium für Biophysikalische Chemie, Technische Universität Berlin, Straße des 17. Juni 135, D-10623 Berlin, Germany*

Received 20 October 2006; received in revised form 14 December 2006; accepted 19 December 2006
Available online 4 January 2007

Abstract

Photosystem II (PSII) is a homodimeric protein–cofactor complex embedded in the thylakoid membrane that catalyses light-driven charge separation accompanied by the oxidation of water during oxygenic photosynthesis. Biochemical analysis of the lipid content of PSII indicates a number of integral lipids, their composition being similar to the average lipid composition of the thylakoid membrane. The crystal structure of PSII at 3.0 Å resolution allowed for the first time the assignment of 14 integral lipids within the protein scaffold, all of them being located at the interface of different protein subunits. The reaction centre subunits D1 and D2 are encircled by a belt of 11 lipids providing a flexible environment for the exchange of D1. Three lipids are located in the dimerization interface and mediate interactions between the PSII monomers. Several lipids are located close to the binding pocket of the mobile plastoquinone Q_B, forming part of a postulated diffusion pathway for plastoquinone. Furthermore two lipids were found, each ligating one antenna chlorophyll *a*. A detailed analysis of lipid–protein and lipid–cofactor interactions allows to derive some general principles of lipid binding pockets in PSII and to suggest possible functional properties of the various identified lipid molecules.

Keywords: Photosystem II; Structure; Lipids; Dimerization; Thylakoid membrane; Plastoquinone diffusion

1. Introduction

The reactions of direct transformation of light into biologically useful chemical energy via oxygenic photosynthesis take place in two multimeric protein–pigment complexes, denoted photosystem I (PSI) and photosystem II (PSII) [1,2], that are anisotropically embedded in the photosynthetic thylakoid membrane of cyanobacteria, green algae and plants. In PSII that catalyses the light-driven oxidation of water, solar energy is captured by pigments in antenna proteins and directed to the primary electron donor P680 of the electron transfer chain where charge separation takes place [3]. The PSII core complex (PSIIcc) from *Thermosynechococcus elongatus* that is deprived during purification of phycobilisome stacks located on the cytoplasmic side of the membrane contains at least 19 protein subunits of which 16 are membrane-intrinsic. The main membrane-intrinsic protein subunits of the PSIIcc are the reaction centre proteins (D1 and D2), the inner antenna proteins (CP47 and CP43), the heterodimeric cytochrome cyt *b-559* (PsbE and PsbF) and a number of low molecular weight proteins of yet unknown function. In cyanobacterial PSII the three membrane extrinsic proteins PsbO (33 kDa), PsbU (12 kDa) and PsbV (cyt *c-550*) are associated at the lumenal side of the core assembly [4].

During the past years, a number of crystal structures of membrane-intrinsic proteins involved in oxygenic photosynthesis have been published: PSI of cyanobacteria [5] and higher plants [6], the cyt b_6f complex of cyanobacteria [7] and algae [8], the plant LHCII [9,10] as well as medium resolution (3.2 Å to 3.8 Å) structures of cyanobacterial PSIIcc [11–14].

A general property of the thylakoid membrane of cyanobacteria, algae and plants is to provide the matrix for photosynthetic protein–pigment complexes (PSII, cyt b_6f, PSI and ATP syntethase) catalysing the reactions of oxygenic photosynthesis [1] and to hinder the free diffusion of ions, a prerequisite for the generation of an electrochemical potential

* Corresponding author. Tel.: +49 30 31421122; fax: +49 30 31425580.
E-mail address: kern@chem.tu-berlin.de (J. Kern).
[1] Current address: Max-Planck-Institut für Medizinische Forschung, Abteilung für Biomolekulare Mechanismen, Jahnstr. 29, D-69120 Heidelberg, Germany.

0005-2728/$ - see front matter © 2007 Published by Elsevier B.V.
doi:10.1016/j.bbabio.2006.12.009

difference across the membrane that drives ATP synthetase. The lipid composition of thylakoid membranes is highly conserved among oxygenic photosynthetic organisms. It is composed of uncharged monogalactosyldiacylglycerol (MGDG; ~50%) and digalactosyldiacylglycerol (DGDG; ~30%), as well as anionic sulfoquinovosyldiacylglycerol (SQDG; ~5–12%) and phosphatidylglycerol (PG; ~5–12%) [15]. The found lipid composition of the thylakoid membrane for a number of thermophylic cyanobacteria is summarized in Table 1. It should be noted that the lipid composition is dependent on the growth conditions, see for example [16]. Because of its high concentration in the thylakoid membranes, MGDG is the most abundant polar lipid species in nature. Compared to the animal, bacterial and non-chloroplastic cellular membranes, which are dominated by the presence of phospholipids, thylakoid membranes contain smaller amounts of phospholipids. The lipid molecules and proteins located in the membrane (membrane-intrinsic) each contribute about 50% of the total thylakoid mass. The high protein-to-lipid ratio is typical for energy converting membranes. A broad overview of the role of lipids in photosynthesis is given in Ref. [17].

From a structural point of view lipid molecules can be divided into three different classes: (i) the bulk lipids in the membrane that interact non-specifically with the proteins; (ii) the annular lipids, that are in direct contact with the outer surface of the membrane embedded proteins; and (iii) the integral (non-annular) lipids, which are found at subunit interfaces within a protein complex. The integral lipids are residing at well-defined positions in the protein complexes and possibly have a specific function for example in folding or assembly of protein subunits. Excellent descriptions of these lipid classes are given in ref [18,19]. The X-ray structures of the above mentioned protein complexes (except for PSIIcc at medium resolution where lipids could not be modelled with confidence) have shown a number of integrally bound (class iii) lipids.

Several biochemical studies highlighted the importance of the different classes of lipid molecules in PSII. It was observed that the pigment content and the photosynthetic activity were reduced in strains having mutations in the biosynthesis pathway of PG and therefore a reduced content of PG [20,21]. In another study the oxygen-evolving activity was reduced by 40% in intact cells after 3 days depletion of PG [22]. This is most likely caused by inhibition of electron transfer from Q_A to Q_B, suggesting that PG is required for maintaining the binding site of Q_B. Fluorescence measurements in mutants of *Arabidopsis thaliana*, which are severely deprived of DGDG, indicate that part of the DGDG molecules are specifically bound and affect predominantly the reaction properties of PSII on the electron donor side [23].

Despite these findings only very limited biochemical information was available so far about positions of lipids within the PSII core complex. For instance, binding studies using lipid-specific antibodies revealed that SQDG is accessible at the outer surface of the D1/D2 heterodimer of tobacco [24], and a tight binding of PG to the membrane intrinsic part of D1 was concluded from lipid analysis of the purified D1 protein [25]. A possible location of PG at the dimerization interface was concluded from phospholipase treatment of dimeric PSII from spinach [26], and a hydrogen-bonding interaction of DGDG with various Tyr residues was found by FTIR studies on DGDG depleted PSII [27].

Recently, our group published the crystal structure of PSIIcc at 3.0 Å comprising 77 cofactors per monomer including, for the first time, 14 integral lipids and three detergent molecules [28]. The total number of 14 identified lipid molecules was unexpectedly high and their locations are remarkable, as some are in close vicinity to redox-active cofactors and others are thought to form part of a hydrophobic diffusion pathway for plastoquinone 9 (PQ9) into and out of the Q_B pocket.

Based on present biochemical and structural data, lipids must have important structural and functional roles in PSIIcc that will be highlighted here with respect to several questions: How do lipid molecules influence the structure of the entire complex and do they regulate protein–protein interactions of different subunits? Do lipids interact with cofactors, perhaps modulating their properties? Do the structurally characterized lipids explain the biochemistry of protein–lipid interactions?

2. Lipid content of cyanobacterial PSII

The lipid and detergent composition of PSIIcc from *T. elongatus* has been analyzed by means of thin layer chromatography (TLC), resulting in ratios of 3 n-dodecyl-β-D-maltoside (β-DM)/chlorophyll *a* (Chl*a*) and 0.56 fatty acids/Chl*a* for dimeric PSIIcc which could be crystallized, as well as 4 β-DM/Chl*a* and 1.0 fatty acids/Chl*a* for monomeric PSII [29], giving a minimum number of 10 lipids/P680 for dimeric PSII and 18 lipids/P680 for monomeric PSII. These numbers have to be treated as lower limits as loss of lipids during the isolation and quantification procedure is likely. This becomes obvious when comparing the found numbers with the number of at least 14

Table 1
Lipid composition of cyanobacterial thylakoid membranes and isolated monomeric and dimeric PSII in comparison to the recent X-ray structure

Sample	Total lipids/P680	MGDG (mol%)	DGDG (mol%)	SQDG (mol%)	PG (mol%)
Structure of dimeric PSIIcc from *T. elongatus* [28]	14	43	29	21	7
Monomeric PSII from *T. elongatus* [30]	18±6	41±6	28±6	16±9	13±5
Dimeric PSII from *T. elongatus* [30]	10±4	37±10	32±10	13±10	18±7
Dimeric PSII from *T. vulcanus* [32]	≈25	29.8±1.0	21.1±2.1	20.4±2.3	28.7±2.3
Thylakoids of thermophilic *Synechococcus* 6716 [60]		≈45	≈23	≈17	≈12
Thylakoids of *T. vulcanus* [16]	–	48±3	32±3	15±3	5±1
Thylakoids of *T. vulcanus* [32]	–	43.5±1.5	25.6±0.2	24.9±1.1	6.1±0.6

lipids/P680 found in our recent X-ray structure. The ratio of the different lipids exhibited some variation between samples. The mean composition for dimeric PSII was 37±10% MGDG, 32±10% DGDG, 13±10% SQDG and 18±7% PG (see Table 1 and [30]).

Using a different purification protocol, Ohno and coworkers determined about 60 lipids/P680 of PSII from *T. elongatus* [31]. Sakurai et al. observed a lipid content of 27 lipids/P680 in PSII from *Thermosynechococcus vulcanus* [32], but found a lipid composition within the purified PSII complexes (30, 21, 20, 29% of MGDG, DGDG, SQDG and PG, respectively) that differs from the composition of the thylakoid membrane of this organism (44, 26, 25, 6% of MGDG, DGDG, SQDG and PG, respectively). A comparison of the results from lipid quantification of various PSII preparations with the found lipid content in our X-ray structure is given in Table 1. The large deviation from the number of 14 lipids identified in the X-ray structure can be explained by the fact that the used analytical methods do not allow to distinguish between free, annular, or integral lipid molecules. The biochemically determined numbers of lipids are therefore highly dependent on the used purification procedure and should be regarded as a rather rough estimate.

3. Characteristics and assignment of lipids in Photosystem II

The electron density maps of *T. elongatus* PSIIcc at 3.0 Å resolution showed elongated features, which could be assigned to phytol chains of Chl*a* and pheophytin *a* (Pheo*a*), to carotenoids (Car), to isoprenoid tails of PQ9 as well as to fatty acid chains of lipids and to dodecyl chains of detergent molecules [28]. These organic moieties fill the volume between the subunits. Still, the difficulty is that the long fatty acid chains of the lipids show a high degree of flexibility and are therefore difficult to model and are often incomplete. In contrast, the lipid head groups could be identified by typical hairpin-shaped features in the electron density within the transmembrane region with the hydrophilic head groups close to both membrane surfaces where they interact with hydrophilic protein side chains (Fig. 1). The assignment of lipid head groups was guided by the size of the respective head group, possible polar interactions between protein and the head group and the assignment of SQDG was supported by electron density for the sulphur atoms from anomalous difference X-ray diffraction data [28].

In total we identified six MGDG, four DGDG, three SQDG, one PG as well as three β-DM molecules per PSIIcc monomer. The composition of the modelled and refined lipid molecules reflects the composition of lipids in the thylakoid membrane and is within the (relatively large) error in agreement with the biochemically determined lipid composition of our purified PSIIcc samples (see Table 1). As the largest deviation between the crystallographically and biochemically determined content is found for PG and a recent study on PSII form *T. vulcanus* revealed an elevated PG content of isolated PSII compared to thylakoid membranes (see Table 1 and [32]) it is likely that at higher resolution one or two additional PG molecules might be identified in the electron density.

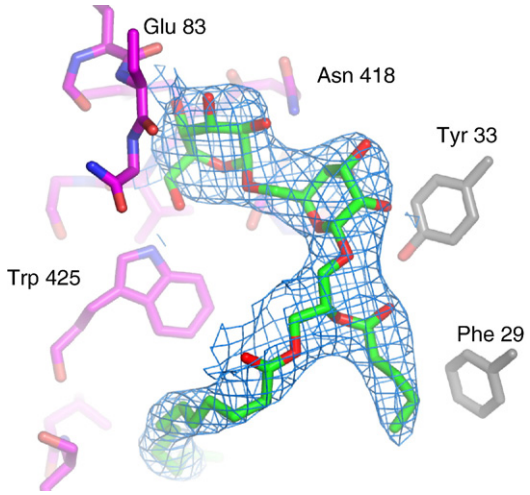

Fig. 1. Example for electron density of a lipid molecule at 3.0 Å resolution. DGDG 5 (green) is shown in stick representation, the $2F_o–F_c$ electron density assigned to the galactolipid is contoured at 1.0 σ level (blue). Selected amino acids of CP43 and PsbJ are shown in magenta and grey, respectively. Hydroxyl groups of the sugar moiety (red) are hydrogen bonded to the protein backbone and to some side chains.

For three reasons we can state that all found lipids are "native" constituents of the PSII complex: (i) we did not add any lipids to our preparation during the purification procedure; (ii) the lipid to protein ratio is extremely decreased during purification, making diffusion of non-native lipids into the protein complex unlikely; and (iii) we observe unambiguous electron density for the head groups of all identified lipids in the structure, therefore a heterogeneity with regard to the nature of the head group can be excluded.

It should be noted that only lipid SQDG 4 could be completely modelled with two hexadecanoic acids, for the other lipids at least half of the acyl chain atoms (assuming an average lipid carrying one hexadecanoic and one octadecanoic acid) could be identified. Their chain length as well as saturation cannot be determined from electron density, maybe partially reflecting the natural heterogeneity of each lipid class with regard to the fatty acid composition or merely a too high degree of flexibility. The hydrophobic fatty acid side chains are anchored in the hydrophobic interior of the complex between transmembrane spanning α-helices (TMH) and mainly stabilized by hydrophobic interactions. However, higher resolution structures of PSIIcc might reveal the presence of additional lipid molecules (see paragraph on unassigned electron density) and in particular the location of annular lipid molecules that could not yet be identified because they are possibly disordered.

A general feature of the lipid binding pockets found in PSII is that the environment of the head groups (about seven to eight amino acids) is different compared to the environment of fatty acid parts. The latter reveal only very few contacts to protein side chains (about one amino acid per fatty acid chain) and are mainly interacting with aliphatic segments of other cofactors (phytol or isoprenoid chains, Car) or with other fatty acid chains in their surrounding (Table 2). The predominant amino acids interacting with the fatty acid chains are Phe, Leu and Trp. This contrasts the amino acids in the binding pockets of the head

Table 2
Overview of lipid and detergent molecules bound to PSII

No.	Lipid type	Orientation of head group	Neighbouring subunits	Protein interaction <=3.5 Å	Neighbouring cofactors head/*tail*
1	MGDG	lumenal	D1, CP43, *Psb*I	A-Phe93, A-Trp97, C-Ser216, I-Lys5Nζ*, I-Tyr9*/C-Phe218, C-Trp223, C-Met281, C-Phe284*	ring Chl*a*7(3.3, 12), head DGDG2 (13)*/ring Chla41 (4.3), phyt Chla33 (7), fa DGDG2 (3.9), Car17 (8)*
2	DGDG	lumenal	D1, CP43	C-Pro217O*, C-Phe218O*, C-Gly220N*/O*, C-Gly222, C-Val225, C-Ser226, C-Asn228Nδ*, C-Cys288, C-Phe292O*, C-Asn294, C-Arg362O*/ *A-Phe155, A-Ile163, C-Phe284, C-Leu438*	ring Chl*a*33 (11.2, 14), ring Chl*a*34 (10.6, 15), ring Chla7 (15.6, 19.9), head MGDG1 (13), Car17 (10.6), heme cytc-550 (23.4, 29.2) Mn_4Ca (15.5)*/fa MGDG1 (3.9), ring Chla41 (5.6)*
3	PG	cytoplasmic	D1, D2, CP43	A-Arg140Nη1[#]/Nη2[#], A-Trp142, A-Phe273, C-Trp36, D-Asn220Nδ*/Oδ*, D-Ala229O[#], D-Thr231Oγ[#], D-Phe232, C-Trp443, C-Arg447Nε*/*A-Ala276, C-Trp36, C-Phe436*	ring Chl*a*44O2D*, O1D*, head SQDG4 (9.2 S-P), Fe (17.1 P-Fe), Q_A (13, 16.9 P-O), Q_B (16, 18.9 P-O)*/fa SQDG4 (3.4), phyt Chla44 (4.1), phyt Chla46 (4)*
4	SQDG	cytoplasmic	D1, D2, CP43	A-Arg233, A-Asn267Nδ*, A-Ser270Oγ*, D-Phe232, D-Arg233, C-Glu29Oε*, C-Trp36Nε*/*C-Trp35*	head PG3 (9.2 S-P), head Q_B (10.2, 17.2 S-O), Q_A (19.3, 22.6 S-O), Fe (15, 19.9 S-Fe), ring Chl*a*44 (13.5, 16.7 S-Mg), ring Chl*a*47 (10.8, 16.1 S-Mg), heme cyt b-559 (23.3, 31.4 S-Fe)*/fa PG3 (3.4), fa MGDG7 (4), phyt Chla44 (3.8), Car12 (4.4), Car11 (7.7), ring Chla47 (9.2)*
5	DGDG	lumenal	D1, CP43, PsbJ	C-Glu83O*, C-Trp425Nε*, C-Val20, C-Ser406Oγ*, C-Asn418Nδ*, J-Tyr33OH*, /*A-Phe197, C-Thr428, J-Phe29*	potential indirect ligand Chl*a*37 (3.2 O-Mg,), head DGDG6*, Mn_4Ca (22), heme cyt c-550 (15.2, 20.3), UNK6 (3.2)*/UNK5 (4.6), ring Chla34 (8.5), phyt Chla37 (3.7), phyt Chla44 (6.6), fa DGDG6 (4.0)*
6	DGDG	lumenal	D1, CP43, PsbJ	A-Asn301, A-Ser305Oγ*, C-Asn415Nδ*, C-Ser416N*, C-Asn418Nδ*, J-Tyr33, J-Ala32O*, J-Gly37O*, V-Gln60*/A-Gln199, A-Leu200, A-Phe300, J-Phe29*	head DGDG5 (2.8*), head MGDG7 (5.4), ring P_{D1} (22), Mn_4Ca (24), heme cyt c-550 (16, 19.6)*/fa MGDG7 (4.0), fa DGDG5 (3.8), phyt Chla44 (4.0), ring Chl_{D2} (5.5), ring Car1 (7.7)*
7	MGDG	lumenal	D2, PsbF, PsbJ	D-Tyr67O*,OH*, D-Gly70O*, F-Met40, F-Gln41Nε*, J-Gly31O*, J-Gly35, J-Gly37*/D-Leu49, D-Phe73, F-Leu26, F-Thr30*	ring DGDG6 (5.4), ring DGDG5 (15), ring Chl_{D2} (17.6, 19), heme cyt b-559 (21, 25), ring P_{D1} (24.7, 25)/*Car11 (3.9 Å), phyt P_{D2} (3.6), phyt Chl_{D2} (3.7), fa DGDG6 (3.6), fa SQD4 (4)*
8	DGDG	lumenal	D2, CP47, PsbH	D-His87N*, D-Ser165O*, B-Tyr193OH*, B-Ser227Oγ*, B-Tyr258, B-Tyr273O*, H-Tyr49, H-Val60O*, H-Trp62N*/Nε*/*B-Phe250, B-Phe463*	ring Chl*a*12 (12.3, 16)*/phyt Chla12 (3.8), phyt Chla21 (4), ring Chla21 (4.2), phyt Chla22 (4.3)*
9	MGDG	cytoplasmic	D2, CP47	D-Arg139Nη*, D-Tyr141OH*, D-Phe269, B-Trp5, B-Tyr6, B-Arg7Nη*, B-Trp468*/B-Phe464*	head MGDG10 (3.4*), ring Chl*a*24 (3.9), MGDG11 (12.5), Fe (16), Q_A (18) Q_B (17)*/phyt Chla26 (4), fa MGDG10 (3.6), phyt Chla17 (4.2)*
10	MGDG	cytoplasmic	D1, D2, CP47, PsbL	A-Ser232, A-Asn234Nδ*, D-Trp266, B-Tyr6OH*, L-Glu11O*, L-Ser16Oγ*, L-Ser16O*/*D-Phe273, L-Gly20*	head MGDG9 (3.4*), head MGDG11 (4.2), head Q_A (17), ring Chl*a*24 (9, 16), Fe (19), ring Chl*a*27 (11, 17)*/phyt Chl_{D1} (3.2), ring Chl_{D1} (6.6), phyt Chla24 (3.8), ring Chla27 (4), phyt Chla26 (4.3), UNK1(3.6), fa MGDG9 (4.5), fa MGDG1 (3.9), tail Q_A (3.9)*
11	MGDG	cytoplasmic	D1, D2, PsbL, PsbT	D-Ile259, D-Ala260O*, D-Phe261, D-Ser262O*/Oγ*, D-Asn263, D-Trp266, L-Thr15Oγ*, L-Leu19*/T-Phe10, T-Phe17*	MGDG10 (4.2, 8), Q_A (7), Fe (13), MGDG9 (8, 14)*/tail Q_A (3.7), fa MGDG10 (3.9), UNK1 (4.2), phyt Chl_{D1}(3.8), phyt $ChlP_{D1}$ (3.6), phyt $Pheo_{D1}$ (4), ring Car4[a] (3.8)*
12	SQDG	cytoplasmic	D1[a], CP47	A-Trp20Nε[a]*, A-Asn26OD[a]*, A-Arg27[a], A-Leu28N[a]*, B-Trp113Nε[#], B-Tyr117OH[#]*/not modelled*	ring Chl*a*29 (6.3, 11.5 S-Mg), Car1[a] (10.4), Car4 (3.5), Car6 (3.5), SQDG13 (15.7 S-S)*/not modelled*
13	SQDG	cytoplasmic	CP47, PsbL, PsbL[a], PsbM[a], PsbT, PsbT[a]	B-Arg18Nη*, L-Arg14Nη[a]*,L-Asn4, L-Tyr18OH[a]*, M-Tyr26[a], T-Phe23O[a]*/*B-Leu29, B-Ser104, PsbT-Phe19[a]*	Car3 (6.5), Car6 (7.2), Car4 (15.5), Chl*a*27 (10.5, 13.7), MGDG11[a] (13.2), MGDG10[a] (15)*/Car3 (4.0), Car4 (4.0) Car5 (3.9), phyt Chla27 (3.9), UNK2[a] (3.9)*
14	MGDG	lumenal	CP47, PsbL, PsbM	B-Thr327Oγ*, B-Phe453, L-Phe35, M-Asn4, M-Leu6	potential indirect ligand of Chl*a*17 (Mg-O 3.9, O1A-O1A 2.6, OBD-O5D 3.2), ring Car3 (3.4), Car4 (7.9), β-DM16[a] (3.2*)*/phyt Chla17 (3.8), ring Car5 (4.3)*
15	β-DM	lumenal	D1, D2, CP47[a]	A-Leu72O*, A-Tyr73OH*, D-Arg304Nη*, B-Ala43O[a]*	head β-DM17*, UNK16 (3.7),*/UNK15 (3.5), UNK14 (6), ring Car1(4.1)*
16	β-DM	lumenal	CP47[a], PsbM, PsbM[a], PsbT	B-Tyr40[a] , M-Met1, M-Gln5Nε2[a]*, M-Leu6[a], T-Ile4	head β-DM16[a]*, head MGDG14[a]*, head β-DM17/*ring Chla17(4.2), ring Car3[a] (4.5), ring Car4[a] (4.5)*
17	β-DM	lumenal	D1, CP47[a], PsbT	A-Leu72, B-Ala43[a], B-Thr44[a], T-Met1N*, T-Ile4*/T-Ala11, T-Ile14*	head β-DM15*, head β-DM216 (4), head MGDG14[a] (6)/*Car4[a] (4.3), Car5[a] (3.6)*

[a] Of the other monomer; fa: fatty acid; phyt: phytol chain; * indicates polar interaction of protein or cofactor with lipid head group. In case of SQDG and PG # indicates polar interaction with phosphate or sulphate group of the lipid. Numbers in parentheses are edge–edge distances in Å to neighbouring cofactors, if two numbers are given the second denotes the center-to-center distance of chlorine rings and lipid headgroup if not stated differently.

groups where Tyr, Asn, Trp, and Arg predominate, and the amino acid composition of the lipid binding pockets differ depending on the kind of head group bound to them. For the negatively charged SQDG and PG a higher number of positively charged Arg residues are present in the binding pocket (1.75 Arg/(SQDG or PG) compared to 0.3 Arg/lipid for the neutral galactolipids). In addition the number of polar contacts, with an average of about four to five contacts between lipid and protein, varies dependent on the kind of head group. PG has seven polar contacts with the protein, SQDG four to five, MGDG about three and DGDG seven on average. These specific differences in the binding pockets could provide means for selection of a specific lipid head group over the other available ones during assembly of the complex. For example it seems likely that DGDG could only be incorporated in binding sites where the protein can provide a sufficiently high number of polar contacts and the negatively charged PG and SQDG are preferentially located in positively charged binding pockets. By contrast, the lower number of amino acids contacting the fatty acid moieties could allow for a lower specificity of the lipid binding and allow the incorporation of lipids with different fatty acid composition into one binding site.

The 14 lipids interact with about 120 amino acid residues from 13 of the 19 subunits of the complex (making contacts to less than 5% of the 2700 amino acids) but form contacts to 23 of the 52 organic non-lipid cofactors (44%) in the complex.

4. Arrangement of lipids in photosystem II

In the 3.0 Å resolution structure of PSIIcc, 11 lipid molecules surround the reaction centre, separating it from the antenna and low molecular weight subunits. The remaining three lipids and the three detergent molecules are located at the monomer–monomer interface (Fig. 2). The head groups of six lipids are located on the cytoplasmic side whereas those of the remaining eight lipids are on the lumenal side. The negatively charged lipids SQDQ and PG are exclusively bound to the cytoplasmic side. This observation follows the asymmetric distribution of positively charged Lys and Arg residues, which are predominantly found towards the cytoplasm, whereas negatively charged Glu and Asp residues are found predominantly on the lumenal side. Positively charged Lys and Arg residues have been frequently identified as coordinating amino acids of the negatively charged headgroups of phospholipids in membrane proteins situated in mitochondrial membranes [33] as well as in the here described structure of PSIIcc.

Several elongated features in the electron density could not be attributed to any specific cofactor and were modelled as

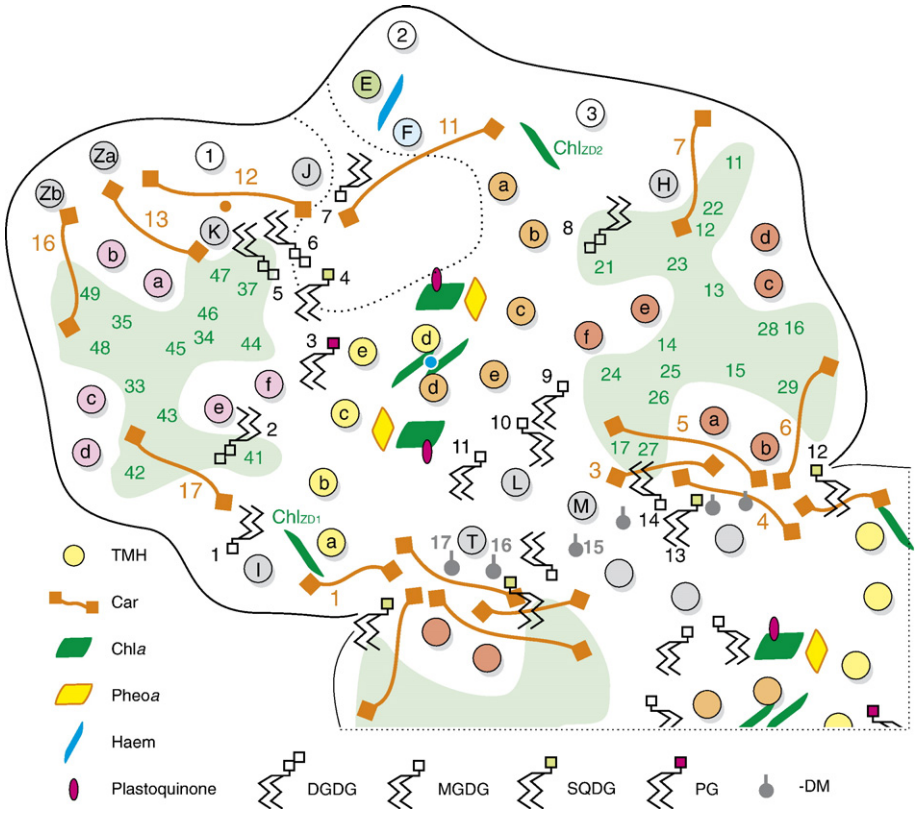

Fig. 2. Schematic arrangement of lipid molecules and other cofactors in the PSII complex. Shown is the membrane-intrinsic part of one PSII monomer viewed from the cytoplasmic side. Transmembrane α-helices (TMH's) are represented as circles, other protein elements are omitted for clarity. The main subunits are highlighted as follows: reaction centre subunits D1 (yellow) and D2 (orange), antenna subunits CP43 (magenta) and CP47 (red), and the α- and β-chain of cytochrome *b-559* (green and cyan, respectively). Low molecular mass subunits are coloured grey. Unassigned TMHs are labelled 1, 2, 3. Symbols for cofactors are given in the figure. The non-haem Fe^{2+} (blue, center of top monomer) and putative Ca^{2+} (orange, top left) ions are shown as spheres. The corresponding numbering is given only for cofactors belonging to the top monomer. Lipid and detergent molecules with headgroups pointing 'downwards' or 'upwards' are located at the lumenal or cytoplasmic side, respectively. Green numbers in CP43 and CP47 indicate the positions of antenna Chl*a*. The Q_B diffusion cavity is indicated by a dotted line.

aliphatic chains (labelled as unknown, "UNK" in the coordinate file). Considering their shapes and positions we expect that some of them belong to not yet identified lipid molecules. Two of these putative lipid sites are located on the cytoplasmic side of the complex: one at the monomer–monomer interface near PsbM and SQDG 13, capable to harbour one lipid molecule, while the second site located between D2 and CP47 subunits and near Chl*a* 21, could accommodate one or two lipids. One lipid molecule may also be expected on the lumenal side of PSIIcc close to DGDG 5 and located in a pocket formed by subunits CP43, PsbJ, PsbK and unassigned subunit X1. If this were a lipid, its headgroup would be located near a putative Ca^{2+} [28] that is coordinated by side chains of PsbK.

5. Lipid belt around the reaction centre

An excess of light can cause chemical damage to PSII as at high light intensities Chl*a* triplet states can be populated and react with molecular oxygen to form singlet oxygen that may lead to oxidative damage of protein subunits and cofactors [34]. The most prone to this damage is subunit D1, which has to be constantly renewed (for a review of D1 turnover see Ref. [35]). Interestingly, the shell of 11 lipid molecules around the reaction centre is asymmetric. Six lipid molecules (MGDG 1, DGDG 2, PG 3, SQDG 4, DGDG 5, and DGDG 6) are located at the interface between D1 and CP43, while only three (DGDG 8, MGDG 9, and MGDG 10) were identified between D2 and CP47 (Fig. 3). The other two lipids (MGDG 7, MGDG 11) are located between D1 or D2 and smaller subunits. Biochemical data show that CP43 is easier disassembled from PSII than CP47 [26], and that it is inserted during a later step of assembly [36]. Removal or motion of CP43 could facilitate the replacement of photo-damaged subunit D1. The increased lipid content at the D1/CP43 side of the complex provides flexible environment and might foster higher mobility of these

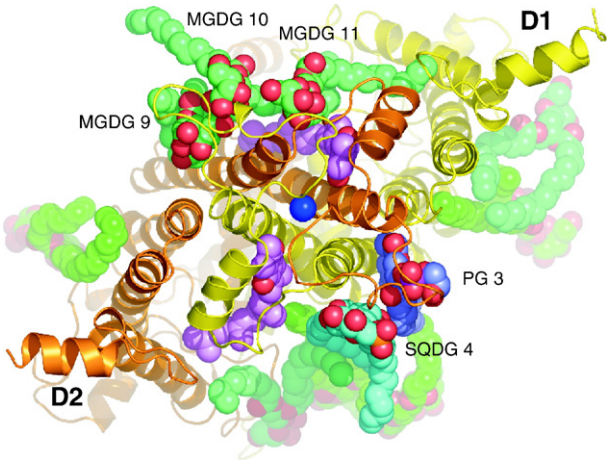

Fig. 3. View of the lipid belt around the reaction centre subunits D1 (yellow) and D2 (orange) of one PSII monomer from the cytoplasmic side. Lipid molecules are drawn in space-filling representation: DGDG (green), MGDG (lime-green), SQDG (cyan) and PG (blue). Lipids in the vicinity of the quinone binding sites are labelled. The non-haem Fe^{2+} (blue) is drawn as sphere and the plastoquinone molecules (violet) are drawn in space-filling representation, all other bound cofactors are not drawn for the sake of clarity.

subunits that is required to achieve rapid replacement of photodamaged D1 by newly synthesized D1.

The reaction centre of PSII (subunits D1 and D2) and subunits L and M of the purple bacterial reaction centre (PbRC) are related in amino acid sequence and in structure [37,38]. Whereas the PbRC is surrounded by spatially separated outer antenna proteins, the so-called light harvesting complexes, the antennae of PSIIcc are formed by the tightly associated protein subunits CP47 and CP43. It is feasible to suggest that the ring of 11 lipids around D1/D2 could resemble the lipid environment around the reaction centre subunits of PbRC. The influence of the lipid composition on the redox potential of Q_A/Q_B was shown by reconstitution of PbRC in liposomes of varied composition [39,40]. It could well be that the inner ring of lipids around the PbRC was conserved during evolution from a simple reaction centre (RC) to the more complex PSII as only part of the hydrophobic membrane lipids surrounding PbRC were replaced by the additional membrane intrinsic subunits in PSII. The presence of the lipid belt might also explain the possibility to biochemically isolate the so-called reaction centre preparations [41] composed of the reaction centre subunits D1 and D2, cyt *b*-559 and the low molecular weight subunit PsbI that are frequently used for spectroscopic studies of PSII.

6. Lipids and detergent at the monomer–monomer interface

The dynamic process of D1 replacement was shown to involve the monomerization of the PSIIcc dimer followed by the release of CP43 [42]. Kruse and coworkers reported the involvement of specific PG molecules in spinach PSII dimer to monomer inter-conversion [26] that provide a high degree of flexibility. Some involvement of PG in the formation of dimeric PSII was also found in studies on a deletion mutant of the biosynthesis pathway for PG in *Synechocystis* PCC 6803. In these mutant cells deprived of PG, the addition of PG was not essential for but accelerated significantly the reformation of dimeric PSII after high light treatment [43].

PG plays also a crucial role in the trimerization of the plant LHCII complex [44]. In the recently determined crystal structure of pea LHCII a PG molecule binds at the monomer–monomer interface [9,10], whereas three DGDG molecules fill a hydrophobic cavity on the three-fold axis near the lumenal side.

In the structure of *T. elongatus* PSIIcc six lipid molecules (SQDG 12, SQDG 13 and MGDG 14 from each of the two monomers) are found at the interface between the two monomers of PSII. Because lipids SQDG 12 and SQDG 13 form polar contacts to subunits from both monomers simultaneously (Table 2), this suggests an important role of these lipids for monomer–monomer interaction.

In addition, six detergent molecules (three per PSII monomer) are located at the monomer–monomer interface and occupy a large cavity located between subunit D1 of one monomer and CP47 of the other monomer and hydrogen bonded to both monomers. When PSII is located in the thylakoid membrane (in the native state), this cavity may be occupied by two or three lipid molecules with headgroups

located near the lumenal side, thereby forming a lipid-rich monomer–monomer interface with a total number of 12 to 14 or more lipids (taking also into account the unassigned electron density, see above).

Lipids might be important for the dimerization process, providing flexibility and allowing for easier dissociation and dimerization of PSIIcc. In contradiction to the suggestion by Kruse and coworkers [26] we could not identify any PG molecule at the monomer–monomer interface. In addition, the localized detergent molecules have their head groups at the lumenal side of the membrane and could not be replaced by a PG that would prefer the positively charged cytoplasmic side. However, we cannot exclude that additional lipids are present on the cytoplasmic side which are not yet resolved in the 3.0 Å electron density (see discussion of un-interpreted density above).

To evaluate the role of PG in our detergent-solubilized dimeric PSIIcc from *T. elongatus*, we performed a lipase assay similar to the one described [26]. In contrast to the observation for spinach [26], no change in the dimer content was observed even after prolonged incubation with phospholipase A2 (data not shown). An analysis of the specific lipid content of our monomeric and dimeric PSIIcc indicated no specific enrichment of PG in the dimeric form compared to the monomeric form (Table 1 and [30]). These results indicate a possible difference of our system compared to plant PSII with regard to the role of PG in dimer stabilization or the accessibility of PG to phospholipase treatment. Nevertheless, an indirect effect of bulk or annular PG molecules on the stability of dimeric PSII, as suggested in [43], cannot be excluded.

7. Lipid molecules in the vicinity of plastoquinone binding pockets

As in several other non-homologous membrane proteins (PSI [5], cyt b_6f- [7,8] and cyt bc_1-complex [45]), lipids are found in the vicinity of quinone binding niches also in PSIIcc. Lipid MGDG 11 is close to the Q_A binding pocket, its sugar ring being ~7 Å away from the quinone ring of Q_A and at approximately the same height of the membrane plane as the quinone rings of Q_A and Q_B. Near the Q_A site two more lipids are found at longer distance from the plastoquinone, MGDG 10 at ~17 Å and MGDG 9 at ~18 Å. Next to the Q_B site two lipid molecules are found, the one closest to Q_B being SQDG 4 with an edge-to-edge distance of ~10.2 Å (sugar ring to quinone ring) and ~17.2 Å distance between sulfate group and quinone ring. The second lipid PG 3 is approximately equidistant to Q_A and Q_B (17–19 Å). The positions of four of these five lipids follow roughly the pseudo-twofold symmetry relating D1 and D2 (Figs. 2,3). Therefore MGDG 9 and MGDG 10 show roughly the same distance to Q_A as their symmetry counterparts PG 3 and SQDG 4 to Q_B.

Compared to the Q_A binding site the binding site of Q_B is more open due to the absence of a symmetry equivalent lipid to MGDG 11, which is closely associated with Q_A (see Figs. 2,3). This difference could be important to facilitate exchange of PQ9 between the Q_B binding site and the diffusion cavity (see below) and ensure tight binding of the non-mobile PQ9 in the Q_A binding site.

Interestingly both acidic lipids PG and SQDG were inferred to be involved in quinone binding and tuning the properties of the PSII electron acceptor side. From analysis of the PSII activity in a *Synechocystis* mutant strain deprived of PG it was concluded that PG is an intrinsic structural component of PSII and is required for the proper functioning of Q_B, maybe located close to the Q_B binding site [46]. As the found PG 3 is about 17 Å from Q_B a direct interaction is not possible, nevertheless both cofactors interact with the same segment from D1 (D1-Leu 271… D1-Leu 275), making an indirect effect of PG deletion upon the binding pocket of Q_B likely. It cannot be excluded that additional PG molecules might be located in the structure at higher resolution – for example in the large quinone exchange cavity – which could interact more directly with Q_B. In a SQDG deficient mutant strain of *C. reinhardtii* the interaction of the Q_B site with artificial electron acceptors was changed, indicating a conformational change due to depletion of SQDG [47] but effects on the PSII donor side were also observed.

The close association of lipids with quinone binding sites in various membrane proteins could represent a general structural feature and provide part of the hydrophobic binding pocket for the very hydrophobic quinones. For instance a phospholipid is found close to the Q_O site in the yeast respiratory cyt bc_1 complex [45] and an SQDG is close to the Q_O binding site in the cyt b_6f complex [7,8]. In the two branches of the electron transfer chain of PSI, the distribution of lipid molecules is asymmetric because a negatively charged PG molecule is close to phylloquinone Q_K-A (10 Å distance between quinone ring and phosphate) and a neutral MGDG is close to Q_K-B (~17 Å) and MGDG 9 at ~18 Å [5]. This suggests a functional role for the PG and MGDG by tuning the electron transfer rates along the two branches in PSI, but the physiological significance of the two electron transfer pathways and their different kinetic properties are still under debate.

8. The quinone exchange cavity

A large internal cavity for plastoquinone diffusion in and out of PSIIcc has been proposed based on the 3.0 Å structure of PSII [28]. The cavity is located close to the Q_B binding site and surrounded by TMH-d and -e of D1 and TMHs of the low molecular weight subunits PsbJ, PsbK and cyt *b-559* (see Fig. 4). The walls of the cavity are coated by hydrophobic amino acids, by phytol chains of P_{D2}, Chl_{D2}, $Pheo_{D2}$, Chl*a* 37, Chl*a* 44 and Chl*a* 46 and the acyl chains of 4 lipids (SQDG 4, DGDG 5, DGDG 6, and MGDG 7). In addition the jonon rings of Car 11 and Car 12 point into the cavity. As elongated fragments of electron density are located in the cavity, it is likely that some more hydrophobic molecules reside within the open space that are too flexible (or disordered) to be traced at the current resolution of the X-ray data. The cavity has a large opening of about 16×16 Å^2 towards the cytoplasmic side and a smaller one with dimensions of about 10×20 Å^2 which is flanked by the TMH of PsbE, PsbF and PsbJ towards the membrane. The latter

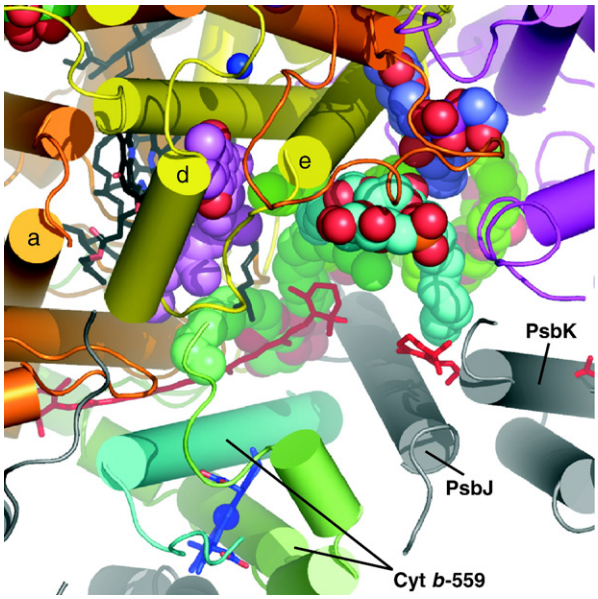

Fig. 4. Lipid molecules decorating the plastoquinone diffusion pathway, view as in Fig. 3. α-helices of protein subunits are shown as cylinders (colouring of subunits D1, D2 as in Fig. 3, α- and β-chain of cyt *b*-559 in green and cyan, remaining α-helices in grey). Lipid and quinone molecules are shown in space-filling representation with the same colour code as in Fig. 3. Other cofactors are in black (Chl*a* and Pheo), orange (Car), blue (haem) drawn as sticks and the non-haem Fe^{2+} (blue) is shown as sphere.

opening suggests that plastoquinone molecules enter the cavity from the bulk membrane phase (from the plastoquinone pool) in oxidized form, and are reduced at the Q_B site which is located opposite this opening at the wall of the cavity. The structures of spinach PSII obtained by electron microscopy [48,49] indicate that the proposed side opening of the cavity into the thylakoid membrane would also be accessible in the plant system and neither hindered by the presence of LHCII nor by the presence of the minor light harvesting complexes CP29, CP26, and CP24.

The central part of the quinone diffusion pathway is large enough to accommodate more than one quinone molecule. Therefore it might serve as a "resting area" for either quinone or quinol molecules. It is noteworthy that a spectroscopic analysis of the chromophores of *T. elongatus* PSIIcc showed the occurrence of about two to three PQ9 per PSIIcc [29]. The presence of a small plastoquinone pool in the solubilized dimeric *T. elongatus* PSIIcc was indicated by flash induced fluorescence measurements [50] and independently confirmed by EPR measurements on PSII from *T. elongatus* by Fufezan et al. [51]. These studies indicate the presence of non-bound PQ9, which could be located either in the diffusion pathway or in the detergent shell surrounding the solubilized PSIIcc.

The postulated exchange of oxidized and reduced plastoquinone between the Q_B site and the plastoquinone pool in the thylakoid membrane via the membrane-facing opening of the cavity is also supported by the recent observation that the isoprenoid chain of ubiquinone in a lipid bilayer system lies in the central part of the bilayer approximately parallel to the membrane plane and does not significantly protrude into the fatty acid region [52]. Similar lipophilic pathways have also been proposed for the photosynthetic cyt b_6f [7,8] and the respiratory cyt bc_1 complex [45].

It is likely that PsbJ and cyt *b-559*, which are flanking the membrane opening, are involved in the regulation of Q_B diffusion. An influence of PsbJ on the electron flow from Q_A to the plastoquinone pool was found in a ΔPsbJ mutant [53]. In another study, it has been shown that the redox potentials of Q_B and cyt *b*-559 are pH-dependent and that the rate of reduction of cyt *b*-559 could be influenced by the conformation of the Q_B site [54]. Since the heme group of cyt *b-559* is exposed to the cavity, this might suggest that conformational changes induced by the contents of the cavity induce switching between the high and low potential state of cyt *b*-559. This is comparable to the sensing mechanism of other cofactors or protein subunits associated with the passage of quinol/quinone along the diffusion pathway that has been proposed for the phytol tail of Chl*a* embedded in the cyt b_6f complex [55].

The large opening of the cavity towards the cytoplasm is most likely filled by several lipid molecules that would shield the interior of the diffusion pathway from the aqueous phase and act as kind of insulator. Based on electron microscopy studies of dimeric PSIIcc and the isolated trimeric allophycocyanin core complex of *T. elongatus*, a patch of low protein density on the cytoplasmic surface of PSII was observed and interpreted as a possible interaction domain with the allophycocyanin antenna proteins [56]. Interestingly the described patch covers the region of the cavity opening on the cytoplasmic membrane surface and it is conceivable that the cytosol-exposed opening is covered by allophycocyanin in the native PSII–phycobilisome complex.

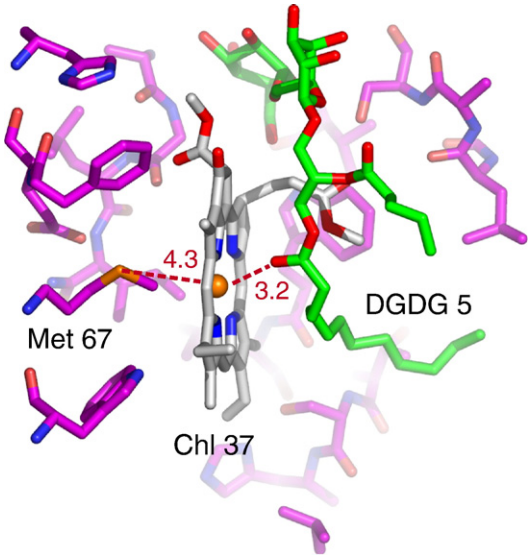

Fig. 5. Ligation of Chl*a* 37 by a lipid molecule. Chl*a* 37 is shown in grey, with oxygen and nitrogen atoms in red and blue, the central Mg^{2+} as orange sphere. The galactolipid DGDG 5 is shown in green, surrounding amino acids from CP43 are coloured magenta. Possible ligation of the central Mg^{2+} by the sulphur atom of CP43-Met 67 or by the acyl-carbonyl of DGDG 5 is indicated by red dashed lines and distances are given in Å. Due to the long sulphur to Mg^{2+} distance ligation of Chl*a* 37 by the protein via CP43-Met 67 is unlikely compared to ligation by the lipid molecule DGDG 5.

9. Interactions between Lipids and Chl*a*

The main interaction between lipid molecules and Chl*a* is the contact between fatty acids and phytol chains. Ten of the lipids reveal such interactions with phytol groups of nine different chlorine moieties (Table 2) and in three cases fatty acid chains point onto the chlorine ring. More interestingly, lipid head groups are observed to be part of the binding pockets for the chlorine rings of five different Chl*a*. Two of these Chl*a* show ligation of the central Mg^{2+} (either direct or indirect) by the lipid head groups and one shows a hydrogen bond interaction between the chlorine ring and the head group of PG 3.

In the antenna subunits, two chlorine moieties located on the lumenal side are in close contact to lipid molecules. The central Mg^{2+} of Chl*a* 17 located in CP47 is at 3.9 Å distance to the acyl-carbonyl function of MGDG 14. In CP43 the acyl-carbonyl of DGDG 5 is at 3.2 Å distance to the central Mg^{2+} of Chl*a* 37 (Fig. 5). Taking into account the long distance and the coordinate error, it is not possible at the moment to decide whether the coordination is direct or via a bridging water. Notably these two lipid molecules were the first to be located in the experimental electron density suggesting that they are embedded in a well-defined binding pocket and have a specific function. Remarkably, these two Chl*a* and lipids are related by the pseudo-twofold symmetry axis that is typical for photosystems and relates both RC subunits as well as the antenna subunits. The described coordination by galacto-lipids represents a novel mode of Chl*a* coordination. To date, similar lipid–chlorophyll binding interactions have been described for PSI [5] and LHCII [9,10] but in these cases the central Mg^{2+} of Chl*a* is coordinated directly by a free oxygen of the phosphodiester group of PG and not by the acyl-carbonyl.

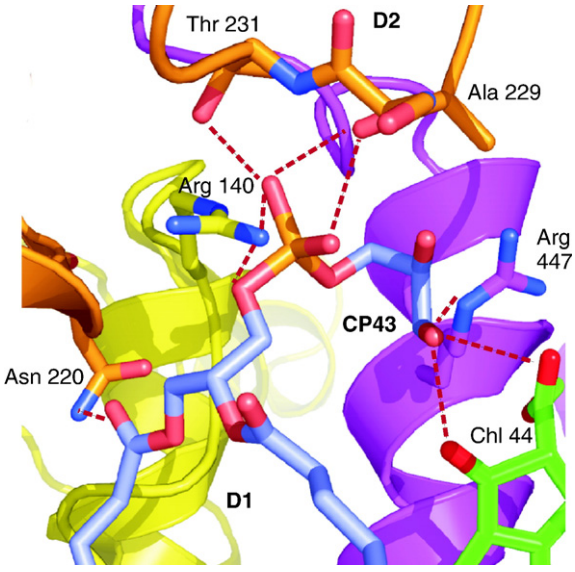

Fig. 6. Binding pocket of the only identified phospholipid, PG 3, shown in stick representation, coloured in blue. The surrounding protein subunits are shown in cartoon representation in yellow (D1), orange (D2) and magenta (CP43) and the closely located Chl*a* 44 in green. Selected amino acids in the binding pocket of the lipid head group are shown and polar interactions of the lipid with protein and Chl*a* 44 are indicated by red dashed lines.

10. Coordination of the PG molecule

The only phospholipid located so far in the structure of *T. elongatus* PSIIcc is PG 3, situated between D1, D2 and CP43. Its negatively charged head group forms polar/hydrogen-bonding interactions with various polar residues, including D1-Arg 140, D2-Asn 220, D2-Thr 231, and CP43-Arg 447 (Fig. 6 and Table 2), thereby mediating the interaction between TMH f of CP43, TMH c of D1 and the de loop of D2. The importance of this interaction is supported by the full conservation of the four residues D1-Arg 140, D2-Asn 220, D2-Thr 231 and CP43-Arg 447 in all known sequences of PSII. A possible hydrogen bond is formed between the glycerol hydroxo group and the 9^1-keto and the carbonyl groups of ring E of Chl*a* 44 (Fig. 6) that contributes to the binding pocket of this antenna Chl*a* and possibly modulates its spectral properties.

11. Other interactions with cofactors

The main form of interactions between different lipids are van der Waals contact between fatty acid chains. These are found between fatty acid chains of 10 of the 14 lipids. In addition, direct hydrogen bonds between the head groups are found for four lipids (between DGDG 5 and DGDG 6 and between MGDG 9 and MGDG 10). Four lipids (MGDG 11, SQDG 12, SQDG 13, MGDG 14) form van der Waals contacts with four different Car (see Table 2). In these cases the lipids contribute directly to the binding pockets of the other cofactors and could therefore be required for proper arrangement/binding of these cofactors.

Various studies indicated changes in PSII activity on the electron donor and acceptor side due to changes of lipid composition in the thylakoid membrane [22,47,57] or by reconstitution experiments of partly delipidised PSII complexes [58,59]. For example an effect of DGDG on the water splitting activity was observed in DGDG depletion mutants of *A. thaliana* [23]. Even though in our structure we do not find evidence for a direct interaction between lipids and the catalytic Mn_4Ca cluster, the closest lipids are DGDG 2 (~15.5 Å), DGDG 5 (~22 Å), and DGDG 6 (~24 Å). This could indicate a more indirect influence of the lipids on the water splitting activity. Possibly conformational changes on the lumenal side of the protein complex are induced when removing a lipid exclusively located on this side of PSIIcc.

12. Conclusions

The crystal structure of *T. elongatus* PSIIcc established lipids to be a new class of cofactors in this and related photosynthetic complexes. Lipid molecules do not only seal PSIIcc in the membrane and couple it with motions of the bulk lipid environment, but lipid–protein and lipid–cofactor interactions in PSIIcc seem to influence the stability of the entire complex and to modulate specifically the functions of protein subunits and cofactors. The prime function of lipids is connected with the flexible nature of their acyl chains that provide deformable interfaces needed for rearrangements of PSIIcc during the

replacement of the photo-damaged components of the reaction centre or transition between monomeric and dimeric states.

Flexible, lipophilic environment provided by fatty acid moieties allows for diffusion of the secondary plastoquinone between its binding site Q_B in PSII and the thylakoid membrane. The lipid headgroups are more rigid and tightly bound to the protein matrix. As an integral part of PSII, they influence the properties (redox potential) of the cofactors of the antenna system and of the electron transfer. The structure of PSIIcc at 3.0 Å resolution provides a basis for the design of well targeted studies on the functional role of selected lipids by genetically modifying their binding pockets.

Acknowledgements

The authors are grateful to Deutsche Forschungsgemeinschaft for support in the frame of Sfb 498 (projects A4, C7), to Fonds der Chemischen Industrie and to the Max Planck Gesellschaft. Beam time and support at ESRF (Grenoble), SLS (Villigen), BESSY (Berlin), and DESY (Hamburg) is gratefully acknowledged. We thank Dr. F. Müh and Prof. G. Renger for critical reading of the manuscript.

References

[1] N. Nelson, A. Ben-Shem, The complex architecture of oxygenic photosynthesis, Nat. Rev., Mol. Cell Biol. 5 (2004) 971–982.
[2] T. Wydrzynski, K. Satoh (Eds.), Photosystem II: The light-driven Water: Plastoquinone oxidoreductase, Springer, Dordrecht, The Netherlands, 2005.
[3] G. Renger, A.R. Holzwarth, Primary Electron Transfer, in: T. Wydrzynski, K. Satoh (Eds.), Photosystem II: The Water/Plastoquinone Oxido-Reductase in Photosynthesis, Kluwer Academic Publishers, Dordrecht, Netherlands, 2005, pp. 139–175.
[4] A. Seidler, The extrinsic polypeptides of Photosystem II, Biochim. Biophys. Acta 1277 (1996) 35–60.
[5] P. Jordan, P. Fromme, H.T. Witt, O. Klukas, W. Saenger, N. Krauss, Three-dimensional structure of cyanobacterial photosystem I at 2.5 Å resolution, Nature 411 (2001) 909–917.
[6] A. Ben-Shem, F. Frolow, N. Nelson, Crystal structure of plant photosystem I, Nature 426 (2003) 630–635.
[7] G. Kurisu, H. Zhang, J.L. Smith, W.A. Cramer, Structure of the cytochrome b6f complex of oxygenic photosynthesis: tuning the cavity, Science 302 (2003) 1009–1014.
[8] D. Stroebel, Y. Choquet, J.L. Popot, D. Picot, An atypical haem in the cytochrome b_6f complex, Nature 426 (2003) 413–418.
[9] Z. Liu, H. Yan, K. Wang, T. Kuang, J. Zhang, L. Gui, X. An, W. Chang, Crystal structure of spinach major light-harvesting complex at 2.72 Å resolution, Nature 428 (2004) 287–292.
[10] J. Standfuss, A.C. Terwisscha van Scheltinga, M. Lamborghini, W. Kuehlbrandt, Mechanisms of photoprotection and nonphotochemical quenching in pea light-harvesting complex at 2.5 A resolution, EMBO J. 24 (2005) 919–928.
[11] A. Zouni, H.T. Witt, J. Kern, P. Fromme, N. Krauss, W. Saenger, P. Orth, Crystal structure of photosystem II from *Synechococcus elongatus* at 3.8 Å resolution, Nature 409 (2001) 739–743.
[12] N. Kamiya, J.R. Shen, Crystal structure of oxygen-evolving photosystem II from *Thermosynechococcus vulcanus* at 3.7-Å resolution, Proc. Natl. Acad. Sci. U. S. A. 100 (2003) 98–103.
[13] K.N. Ferreira, T.M. Iverson, K. Maghlaoui, J. Barber, S. Iwata, Architecture of the photosynthetic oxygen-evolving center, Science 303 (2004) 1831–1838.
[14] J. Biesiadka, B. Loll, J. Kern, K.-D. Irrgang, A. Zouni, Crystal structure of cyanobacterial photosystem II at 3.2 Å resolution: a closer look at the Mn-cluster, Phys. Chem. Chem. Phys. 6 (2004) 4733–4736.
[15] N. Murata, P.-A. Siegenthaler, Lipids in Photosynthesis: An Overview, in: P.-A. Siegenthaler, N. Murata (Eds.), Lipids in Photosynthesis: Structure, Function and Genetics, Kluwer Academic Publishers, Dordrecht, The Netherlands, 1998, pp. 1–20.
[16] L.L. Kiseleva, I. Horvath, L. Vigh, D.A. Los, Temperature-induced specific lipid desaturation in the thermophilic cyanobacterium *Synechococcus vulcanus*, FEMS Microbiol. Lett. 175 (1999) 179–183.
[17] P.A. Siegenthaler, N. Murata (Eds.), Lipids in Photosynthesis: Structure, Function and Genetics, Kluwer, Dordrecht, The Netherlands, 1998.
[18] A.G. Lee, How lipids affect the activities of integral membrane proteins, Biochim. Biophys. Acta 1666 (2004) 62–87.
[19] H. Palsdottir, C. Hunte, Lipids in membrane protein structures, Biochim. Biophys. Acta 1666 (2004) 2–18.
[20] N. Sato, M. Hagio, H. Wada, M. Tsuzuki, Requirement of phosphatidylglycerol for photosynthetic function in thylakoid membranes, Proc. Natl. Acad. Sci. U. S. A. 97 (2000) 10655–10660.
[21] H. Hartel, H. Lokstein, P. Doermann, B. Grimm, C. Benning, Changes in the composition of the photosynthetic apparatus in the galactolipid-deficient dgd1 mutant of *Arabidopsis thaliana*, Plant Physiol. 115 (1997) 1175–1184.
[22] M. Hagio, Z. Gombos, Z. Varkonyi, K. Masamoto, N. Sato, M. Tsuzuki, H. Wada, Direct evidence for requirement of phosphatidylglycerol in photosystem II of photosynthesis, Plant Physiol. 124 (2000) 795–804.
[23] R. Steffen, A.A. Kelly, J. Huyer, P. Doermann, G. Renger, Investigations on the reaction pattern of photosystem II in leaves from *Arabidopsis thaliana* wild type plants and mutants with genetically modified lipid content, Biochemistry 44 (2005) 3134–3142.
[24] R. Voβ, A. Radunz, G.H. Schmid, Binding of lipids onto polypeptides of the thylakoid membrane: I. Galacto-lipids and sulfolipids as prosthetic groups of the core peptides of the photosystem II complex, Z. Naturforsch. 47c (1992) 406–415.
[25] O. Kruse, G.H. Schmid, The role of phosphatidylglycerol as a functional effector and membrane anchor of the D1-core peptide from photosystem II-particles of the cyanobacterium *Oscillatoria chalybea*, Z. Naturforsch. 50c (1995) 380–390.
[26] O. Kruse, B. Hankamer, C. Konczak, C. Gerle, E. Morris, A. Radunz, G.H. Schmid, J. Barber, Phosphatidylglycerol is involved in the dimerization of Photosystem II, J. Biol. Chem. 275 (2000) 6509–6514.
[27] I.S. Gabashvili, A. Menikh, J. Segui, M. Fragata, Protein structure of photosystem II studied by FT-IR spectroscopy. Effect of digalactosyldiacylglycerol on the tyrosine side chain residues, J. Mol. Struct. 444 (1998) 123–133.
[28] B. Loll, J. Kern, W. Saenger, A. Zouni, J. Biesiadka, Towards complete cofactor arrangement in the 3.0 Å resolution structure of photosystem II, Nature 438 (2005) 1040–1044.
[29] J. Kern, B. Loll, C. Lüneberg, D. DiFiore, J. Biesiadka, K.D. Irrgang, A. Zouni, Purification, characterisation and crystallisation of photosystem II from *Thermosynechococcus elongatus* cultivated in a new type of photobioreactor, Biochim. Biophys. Acta 1706 (2005) 147–157.
[30] J. Kern, Structural and functional investigations of Photosystem II from *Thermosynechococcus elongatus*, Dissertation, Faculty II, Technical University, Berlin, 2005.
[31] T. Ohno, K. Satoh, S. Katoh, Chemical composition of purified oxygen-evolving complexes from the thermophilic cyanobacterium *Synechococcus* sp, Biochim. Biophys. Acta 852 (1986) 1–8.
[32] I. Sakurai, J.R. Shen, J. Leng, S. Ohashi, M. Kobayashi, H. Wada, Lipids in oxygen-evolving Photosystem II complexes of cyanobacteria and higher plants, J. Biochem. (Tokyo) 140 (2006) 201–209.
[33] C. Hunte, Specific protein–lipid interactions in membrane proteins, Biochem. Soc. Trans. 33 (2005) 938–942.
[34] A. Krieger-Liszkay, Singlet oxygen production in photosynthesis, J. Exp. Bot. 56 (2005) 337–346.
[35] E. Baena-Gonzalez, E.M. Aro, Biogenesis, assembly and turnover of photosystem II units, Philos. Trans. R. Soc. Lond., Ser. B Biol. Sci. 357 (2002) 1451–1459.
[36] A. Rokka, M. Suorsa, A. Saleem, N. Battchikova, E.M. Aro, Synthesis and

assembly of thylakoid protein complexes. Multiple assembly steps of photosystem II, Biochem. J. 388 (2005) 159–168.
[37] H. Michel, J. Deisenhofer, Relevance of the photosynthetic reaction center from purple bacteria to the structure of photosystem II, Biochemistry 27 (1988) 1–7.
[38] W.D. Schubert, O. Klukas, W. Saenger, H.T. Witt, P. Fromme, N. Krauss, A common ancestor for oxygenic and anoxygenic photosynthetic systems: a comparison based on the structural model of photosystem I, J. Mol. Biol. 280 (1998) 297–314.
[39] L. Nagy, F. Milano, M. Dorogi, A. Agostiano, G. Laczko, K. Szebenyi, G. Varo, M. Trotta, P. Maroti, Protein/lipid interaction in the bacterial photosynthetic reaction center: phosphatidylcholine and phosphatidylglycerol modify the free energy levels of the quinones, Biochemistry 43 (2004) 12913–12923.
[40] L. Rinyu, E.W. Martin, E. Takahashi, P. Maroti, C.A. Wraight, Modulation of the free energy of the primary quinone acceptor (QA) in reaction centers from *Rhodobacter sphaeroides*: contributions from the protein and protein–lipid(cardiolipin) interactions, Biochim. Biophys. Acta 1655 (2004) 93–101.
[41] O. Nanba, K. Satoh, Isolation of a photosystem II reaction center consisting of D-1 and D-2 polypeptides and cytochrome b-559, Proc. Natl. Acad. Sci. U. S. A. 84 (1987) 109–112.
[42] R. Barbato, G. Friso, F. Rigoni, F. Dalla Vecchia, G.M. Giacometti, Structural-changes and lateral redistribution of Photosystem-II during donor side photoinhibition of thylakoids, J. Cell Biol. 119 (1992) 325–335.
[43] I. Sakurai, M. Hagio, Z. Gombos, T. Tyystjarvi, V. Paakkarinen, E.M. Aro, H. Wada, Requirement of phosphatidylglycerol for maintenance of photosynthetic machinery, Plant Physiol. 133 (2003) 1376–1384.
[44] S. Nussberger, K. Dörr, D.N. Wang, W. Kuehlbrandt, Lipid–protein interactions in crystals of plant light-harvesting complex, J. Mol. Biol. 234 (1993) 347–356.
[45] C. Lange, J.H. Nett, B.L. Trumpower, C. Hunte, Specific roles of protein–phospholipid interactions in the yeast cytochrome bc1 complex structure, EMBO J. 20 (2001) 6591–6600.
[46] Z. Gombos, Z. Varkonyi, M. Hagio, M. Iwaki, L. Kovacs, K. Masamoto, S. Itoh, H. Wada, Phosphatidylglycerol requirement for the function of electron acceptor plastoquinone Q(B) in the photosystem II reaction center, Biochemistry 41 (2002) 3796–3802.
[47] A. Minoda, K. Sonoike, K. Okada, N. Sato, M. Tsuzuki, Decrease in the efficiency of the electron donation to tyrosine Z of photosystem II in an SQDG-deficient mutant of *Chlamydomonas*, FEBS Lett. 553 (2003) 109–112.
[48] B. Hankamer, E. Morris, J. Nield, C. Gerle, J. Barber, Three-dimensional structure of the Photosystem II core dimer of higher plants determined by electron microscopy, J. Struct. Biol. 135 (2001) 262–269.
[49] A.E. Yakushevska, W. Keegstra, E.J. Boekema, J.P. Dekker, J. Andersson, S. Jansson, A.V. Ruban, P. Horton, The structure of photosystem II in Arabidopsis: localization of the CP26 and CP29 antenna complexes, Biochemistry 42 (2003) 608–613.
[50] K. Zimmermann, M. Heck, J. Frank, J. Kern, I. Vass, A. Zouni, Herbicide binding and thermal stability of Photosystem II Isolated from *Thermosynechococcus elongatus*, Biochim. Biophys. Acta 1757 (2006) 106–114.
[51] C. Fufezan, C.X. Zhang, A. Krieger-Liszkay, A.W. Rutherford, Secondary quinone in photosystem II of *Thermosynechococcus elongatus*: semiquinone-iron EPR signals and temperature dependence of electron transfer, Biochemistry 44 (2005) 12780–12789.
[52] T. Hauss, S. Dante, T.H. Haines, N.A. Dencher, Localization of coenzyme Q10 in the center of a deuterated lipid membrane by neutron diffraction, Biochim. Biophys. Acta 1710 (2005) 57–62.
[53] I. Ohad, C. DalBosco, R.G. Herrmann, J. Meurer, Photosystem II proteins PsbL and PsbJ regulate electron flow to the plastoquinone pool, Biochemistry 43 (2004) 2297–2308.
[54] C.A. Buser, B.A. Diner, G.W. Brudvig, Photooxidation of cytochrome b559 in oxygen-evolving photosystem II, Biochemistry 31 (1992) 11449–11459.
[55] W.A. Cramer, J. Yan, H. Zhang, G. Kurisu, J.L. Smith, Structure of the cytochrome b6f complex: new prosthetic groups, Q-space, and the 'hors d'oeuvres hypothesis' for assembly of the complex, Photosynth. Res. 85 (2005) 133–143.
[56] J. Barber, E.P. Morris, P.C. da Fonseca, Interaction of the allophycocyanin core complex with photosystem II, Photochem. Photobiol. Sci. 2 (2003) 536–541.
[57] A. Minoda, N. Sato, H. Nozaki, K. Okada, H. Takahashi, K. Sonoike, M. Tsuzuki, Role of sulfoquinovosyl diacylglycerol for the maintenance of photosystem II in *Chlamydomonas reinhardtii*, Eur. J. Biochem. 269 (2002) 2353–2358.
[58] K. Gounaris, D. Whitford, J. Barber, The effect of thylakoid lipids on an oxygen-evolving Photosystem II preparation, FEBS Lett. 163 (1983) 230–234.
[59] K. Akabori, A. Imaoka, Y. Toyoshima, The role of lipids and 17-kDa protein in enhancing the recovery of O_2 evolution in cholate-treated thylakoid membranes, FEBS Lett. 173 (1984) 36–40.
[60] H.S. van Walraven, E. Koppenaal, H.J.P. Marvin, M.J.M. Hagendoorn, R. Kraayenhof, Lipid specificity for the reconstitution of well-coupled ATPase proteoliposomes and a new method for lipid isolation from photosynthetic membranes, Eur. J. Biochem. 144 (1984) 563–569.